CHEMICAL ENGINEERING TRANSACTIONS
VOL. 53, 2016
A publication of AIDIC
The Italian Association of Chemical Engineering
Online at www.aidic.it/cet
Guest Editors: Valerio Cozzani, Eddy De Rademaeker, Davide Manca

ISBN 978-88-95608-44-0; **ISSN** 2283-9216
DOI: 10.3303/CET1653013

Consequences of Liquid Jet Breakup Resulting from Interaction with Overpressure Wave from Domino Effect

Pierre Lauret*[a], Frédéric Heymes[a], Pierre Slangen[a], Laurent Aprin[a], Nicolas Lecysyn[b]

[a]Laboratoire de Génie de l'Environnement Industriel (LGEI), Ecole des Mines d'Alès, Alès, France
[b]CEA, DAM, GRAMAT, F-46500 Gramat, France
pierre.lauret@mines-ales.fr

Storage tanks located on industrial sites are potential source term for leakages, followed by various consequences depending on the nature of the commodity: atmospheric dispersion, BLEVE, UVCE, toxic dispersion. Indeed, because of economic and security purposes, chemical substances are stored with different conditions of pressure, temperature and state. This study explores the consequences of a sudden opening of a storage tank due to an external aggression as a consequence from a previous event. Fragmentation of jets and droplets following the trigger event are thus evaluated. Indeed, increasing the exchange surface impacts the evaporation rate and can be an issue in case of toxic or flammable vapor. Laboratory experiments consisted in generating shockwave with an open ended shock tube to breakup liquid droplets with different viscosities. Size of fragmented droplets are optically measured by direct shadowgraphy. Shockwave is measured using both overpressure sensors and Edgerton retroreflective shadowgraphy. In these experiments, secondary breakups of a droplet into an important number of smaller droplets because of the shockwave induced flow are performed. Results are discussed in terms of velocity and size of droplets. Comparisons are made with existing fragmentation models such as Pilch and Erdman (1987) to provide up to date data with situations encountered in industrial risk evaluation.

1. Introduction

Aggressions on a storage tank of liquid imply loss of containment of the material contained (liquid or gas). Depending on the characteristics of the stored fluid, it can lead to a slow emptying, a jet, rain out and evaporation or direct vaporization. In the last two cases, fragmentation of the liquid occurs. One important question is the behavior of fragmented droplets. Indeed, while the relative velocity of the flow is increasing, the fragmented droplets decrease in diameters. It can lead to complete vaporization of the liquid phase. In order to perform a hazard analysis of a liquid release, convenience is to consider that the whole liquid reaches the ground. Evaporation of the liquid pool is thus studied. Another convenient option is to consider that the whole volume is airborne and disperses in the atmosphere. Therefore, the first assumption shows little hazard, because evaporating rate is generally low whereas the second assumption may give a significant hazard because the whole volume is involved in the vapor phase. Dunbar et al. (1984) have illustrated the complete chain of events from the atomization of a spray after an accidental release to the plume spreading due to atmospheric turbulence. In this work, the goal is to evaluate droplets distribution as a consequence of droplet breakup by shockwave that may occur in case of domino effects in the industry after primary event has caused tank failure. This characterization is prior to the study of droplets evaporation that may lead to toxic dispersion or vapor cloud explosion

2. Literature review

2.1 Catastrophic tank failure

Industrial tank catastrophic failure might have several causes. Salzano et al. (2012) have studied the impact of explosions on tank failure. In this study, focus is made on projectile impact from previous event or external

Please cite this article as: Lauret P., Heymes F., Slangen P., Aprin L., Lecysyn N., 2016, Consequences of liquid jet breakup resulting from interaction with overpressure wave from domino effect, Chemical Engineering Transactions, 53, 73-78 DOI: 10.3303/CET1653013

aggression. Two steps are generally observed when a projectile reaches a tank. The first one is the hydraulic ram: once the projectile enters the tank, there is a sudden and violent release of energy, which generates a shockwave. The second one last the time during the projectile crosses the fluid. An additional exchange of energy, small but of longer duration than the impact one is realized. The cavity formed by the projectile leads to liquid ejection and primary breakup of the jet. Lecysyn et al. (2009) note that liquid ejection leads to catastrophic droplets fragmentation with velocity thirty times less than impact velocity. Moreover, the liquid contained in these droplets is then falling to the ground. In this study we propose to evaluate the behaviour of such a jet when an overpressure wave from domino effect interacts. Heymes (2014) has suggested that consequences of combined aggression may vary a lot depending on the synchronism of escalation vector. The following laboratory study uses calibrated overpressure wave from Open Ended Shock Tube (OEST) and single droplets.

2.2 Pressure and velocity profile behind shockwave

Many hazardous phenomena imply shockwaves such as pyrotechnic explosion, BLEVE, UVCE, pneumatic explosions. In this work, repeatable shockwaves are used through the use of an OEST, described in paragraph 3.1. A shockwave is associated to a wave travelling at higher speed than the speed of sound, resulting in a discontinuity in flow variables (pressure, density, and temperature). In case of explosion, figure 1 represents the dynamic pressure versus time at a fixed location. One can see the discontinuity of dynamic pressure at the shock front followed by a decrease of pressure, a negative phase finally returning to equilibrium.

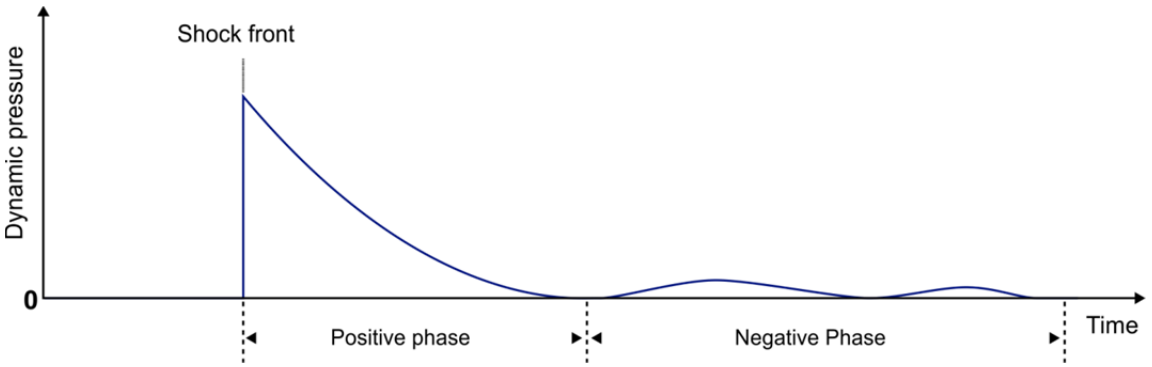

Figure 1: Dynamic pressure profile behind a shockwave at a constant location

Dynamic pressure q is defined as $q = \frac{1}{2}\rho v^2$ with ρ the density of the fluid and v the velocity of the flow. It is proportional to the square of the velocity. Consequently, we cannot assume a stationary flow when dealing with droplets fragmentation induced by a shockwave. Thus, it is very important to characterize the flow through both time and distance in our experiment.

2.3 Droplets breakup by overpressure wave

Droplets breakup is a well-documented phenomenon because of its applications in diesel engines, agriculture, combustion, aerospace industry. At the equilibrium, shape of a droplet is spherical, because it minimizes the surface to volume ratio. When the flow pressure impact the droplet, deformation starts: Rayleigh-Taylor instabilities divide the front of the drop while stripping is done on the sides until fragmentation is achieved. Weber dimensionless number Eq(1) is used to define ratio between dynamic pressure of the flow (using the density of the gaseous phase ρ_g, the relative velocity ΔV) and surface tension σ of the initial droplet d_0 :

$$We = \frac{\rho_g(\Delta V^2)d_0}{\sigma} \quad (1)$$

Viscosity of the fluid μ_l, as the surface tension has an opposite influence on the mechanism of fragmentation compared to the flow inertia. Ohnesorge number, measures this influence:

$$Oh = \frac{\mu_l}{(\rho_l d_0 \sigma)^{1/2}} \quad (2)$$

For a viscosity of 0.1, Pilch and Erdman (1987) had describes three regimes of fragmentation, from We<12 with vibrational breakup to catastrophic breakup at a Weber number superior to 350. Hsiang and Faeth (1995) deepened this work by testing several viscosities, surface tensions and flow velocities. It appears that for a small number of Ohnesorge (<0.1), breakup mode is only influenced by the Weber number.

To evaluate the risk induced by a cloud formed by a jet fragmentation, it is necessary to know the mass median fragment sizes before considering evaporation. Pilch and Erdman define the mass median fragment size as twice the value of the maximum fragment size. This one is evaluated through the use of the critical Weber number We_c, defined as the Weber number under which no fragmentation is observed. According to Guildenbecher (2009), critical Weber number is equal to 12 for Ohnesorge number less than 0.1. Therefore, maximum stable diameter is deduced from Weber number formula:

$$d = We_c \frac{\sigma}{\rho V^2}\left(1 - \frac{V_d}{V}\right)^{-2} \quad (3)$$

A second term is added to take into account for the fragment acceleration. $\boldsymbol{V_d}$ corresponds to the velocity of the cloud of fragments when total breakup time T is reached. Correlation for total breakup time depends on Weber number. In the following, the aim is to validate these correlations for droplet breakup from shockwave interaction by visualisations techniques.

2.4 Flow visualisations techniques

In this paper, different techniques of flow visualization are used. These techniques are based on deviation of the light rays from modification of the refractive index. This refractive index change is due to modification of the density of the flow. The shock front presents an important increase in density that can be emphasized. Shadowgraphy responds to the second spatial derivative of the refractive index and is largely described by Settles (2001). Direct shadowgraphy is used in this work to emphases the droplet fragmentation. Retroreflective Edgerton shadowgraphy, described by Hargather (2009) is used to capture the shockwave at the end of the shock tube. Finally, Particle Image Velocimetry is also used here to characterize the flow behind the shockwave before inserting droplets in the flow.

3. Experimental setup

3.1 Open Ended Shock Tube

The Open Ended Shock Tube (OEST) used in this study is a shock tube composed of a driver section filled with pressurized air until aluminium rupture disk pressure is reached (6.2 absolute bar for 0.2 mm thickness). The driven section is open at the right end. In this work, both sections are 0.15 m diameter large. Dimensions are reported on figure 2. The droplet generator is placed at the exhaust of the driven section. It is used to generate drops from 0.8 mm to 1.8 mm. Temperature and pressure are recorded in the driver section. Three dynamic sensors of total pressure (PCB 102A06 type) are disposed along the driven section. Two others are located in the free field, near the end of the tube, on the outlet axis. High speed data acquisition is realized with 250 kHz sampling.

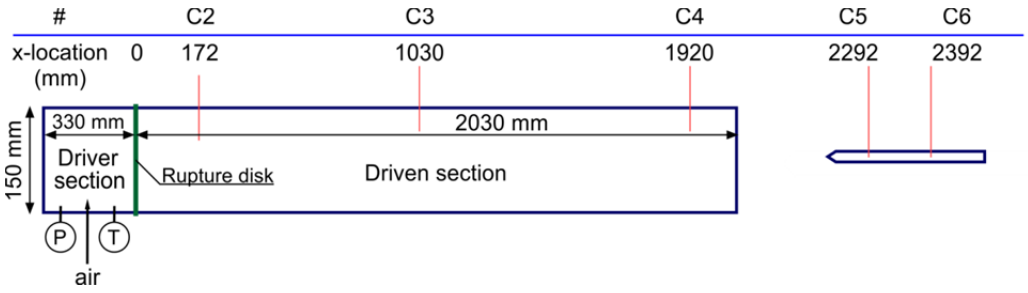

Figure 2: Shock tube configuration with sensors

The flow and the fragmentation are visualised using two Phantom V711 high speed camera. Fragmentation is recorded with direct shadowgraphy using backlighting of the droplets with collimated light beam at 22 000 frame per second (fps) on a field of view of 29.3 mm wide by 39 mm long with resolution of 61 µm/pixel. Camera configurations and specifications are further discussed in previous research paper (Slangen, 2012, 2015 & 2016).

3.2 Droplets fragmentation

The droplet generator is made of an automatic syringe pusher filled with water. Syringe is linked to a 0.84 mm diameter nozzle. The distance between the nozzle and the tube is 30.7 mm, centered and 150 mm height from the tube axis. Continuous drops train ensures the interaction of falling drops with the shockwave as trigging the rupture is not enabled.

4. Results

4.1 Flow measurements

Intensity and velocity of the shockwave are extracted from pressure sensors and high speed imaging analysis and reported on figure 3.

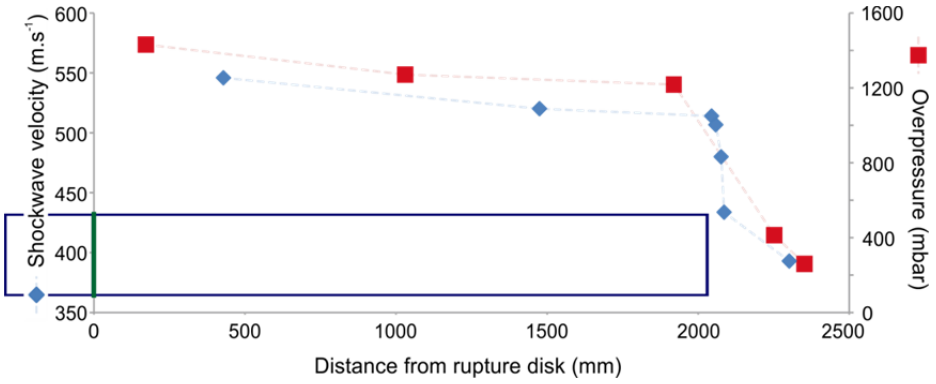

Figure 3: Shock tube velocity and overpressure over distance from rupture disk

Important decrease in overpressure and shock velocity can be observed at the exit of the OEST. In order to characterize precisely the flow impacting the droplets, particle image velocimetry has been used. Velocity of the flow at the distance of falling droplets from the exit of OEST is measured from 200 $m.s^{-1}$ to 300 $m.s^{-1}$. Figure 4 illustrates the sudden increase in dynamic pressure due to overpressure. Time measurement starts when the shockwave exit the shock tube.

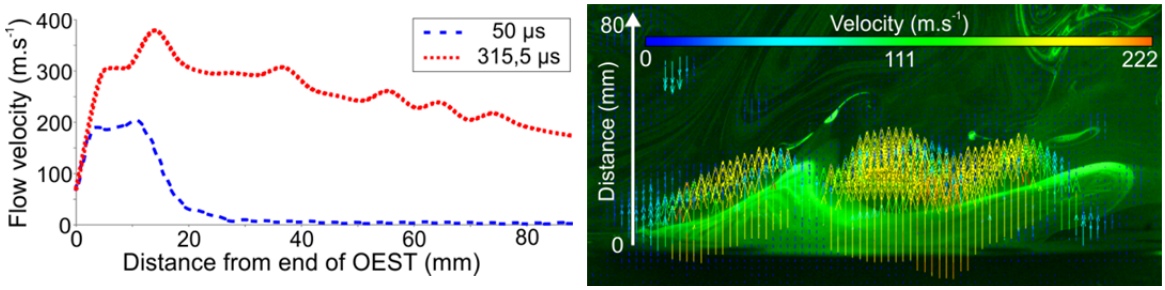

Figure 4: Flow velocity at different time after exit from OEST (left) – PIV analysis extraction at 50 µs (right).

4.2 Droplets fragmentation analysis

Analysis of four droplets from 0.8 mm to 1.47 mm shows a catastrophic breakup with Weber number from 1191 to 2679. Figure 5 shows images of a 0.8 mm droplet fragmentation taken with a time step of 45 µs.

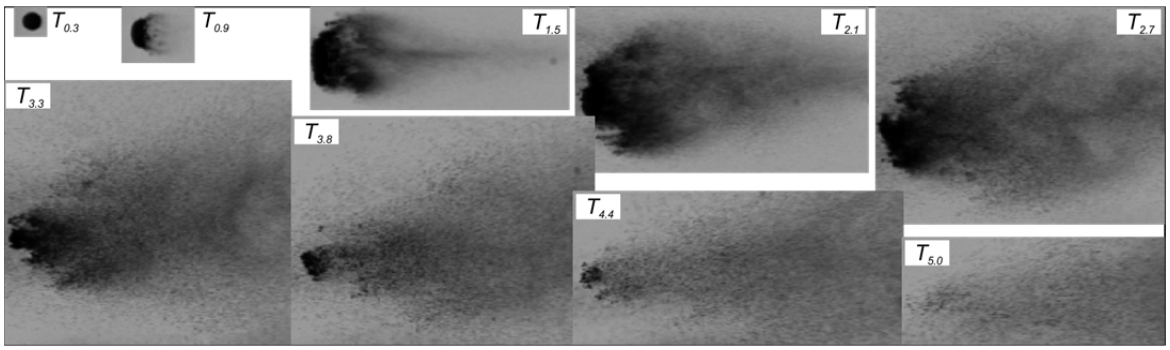

Fiugure. 5: Fragmentation of a 0.8 mm diameter droplet at different dimensionless time.

First image is grabbed when the shockwave reaches the droplet. On the first images, the droplet is deformed by the flow and stripping is beginning on the sides. Then, small perturbations appear on the windward surface of the drop. Finally, large amplitude surface waves penetrate the droplet, also observed by Lee (1999) and Joseph (2000). The wake of the drop is composed of a mist with drop sizes less than the pixel dimension (61 µm).
In this range of Weber number, total breakup time is defined by the following expression:

$$T = 0.766(We - 12)^{0.25} \quad (4)$$

Displacement and velocity correlation are given by:

$$\frac{x}{D} = \frac{3}{8}C_d T^2 + BT^3 \quad (5)$$

$$\frac{V_d}{V\epsilon^{0.5}} = \frac{3}{4}C_d T + BT^2 \quad (6)$$

V_d is the velocity of the fragment cloud when the breakup process has ceased. In the experimental work, this velocity is measured for the stagnation point. ϵ is the flow field/drop density ratio. C_d is the drag coefficient of a rigid constant-mass sphere and *B* is an empirical constant set to 0.116 in compressible flow to take into account the drop deformation. Figure 6 shows that both displacement and velocity are correctly modelled with this approach.

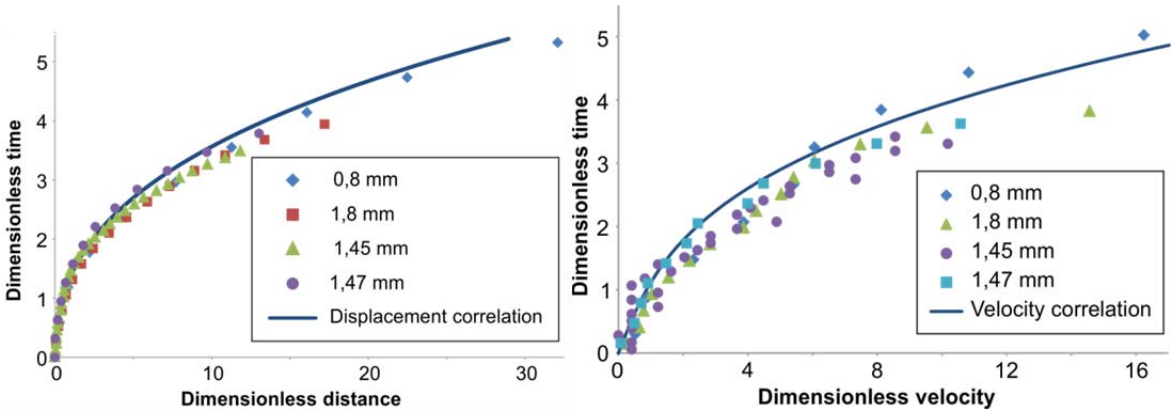

Figure 6: Displacements (left) and velocities (right) of four droplets from 0.8 mm to 1.47 mm compared to theory.

Droplet velocity V_d at the total time breakup *T* is evaluated from the theory and used in (3) to compute the maximum stable diameter d of the fragments. Values are included in the range [20-34] µm depending on the initial drop, leading to a mass median diameter ranges between [10-17] µm. These values obtained from the theory cannot be validated by the camera because of the minimum pixel size (32 µm/pxl) is above. Nevertheless, future experiments require the use of Phase-Doppler Anemometry (PDA) in order to validate the range [10-120] µm. Using values obtained from theory leads to investigate the surface to volume ratio between the initial droplet and the cloud of fragments in a first approach. Hypotheses are as follow:

- During the fragmentation, no evaporation occurs;
- Fragment sizes are uniform, with values equal to sphere with volume calculated from the mass median diameter. PDA experiments in the future are required to investigate the truthfulness of these assumptions.

Number of fragments size is evaluated from 550 000 to 1 250 000 depending on the initial diameter. Thus, considering that during the time of the fragmentation no evaporation occurs, the water volume is constant but the surface area changes. For initial droplets of diameter *d* considered here, exchange surface S_l increases by a factor from 81 to 108. The impact of this variation is important on the mass evaporation rate $\dot{m}$, as one can see on the following equation proposed by Guella (2008):

$$\dot{m} = S_l \frac{Sh_g D_g}{d} \rho_g \left(Y_{v,S} - Y_{v,\infty}\right) \quad (7)$$

Sh_g is the Sherwood number of the gaseous phase. D_g is the vapour diffusion coefficient in air. ρ_g is the gas density. $Y_{v,S}$ and $Y_{v,\infty}$ are respectively the vapour mass fraction near and away from the drop. Analysis of this

equation shows that the mass evaporation rate increases proportionally to the surface and is inversely proportional to the droplet diameter. Therefore, considering on one hand the initial drop and on the other the fragments, mass evaporation rate increases in the second case. Nevertheless, the evaporation rate is modified by the value $Y_{v,\infty}$ that may be not negligible. More work has to be done on the spray evaporation.

5. Conclusions

Storage tank leakage by projectile impact leads to liquid ejection with primary breakup. In the scope of domino effects on an industrial site, explosion from a secondary event can lead to droplet/shockwave interaction. This interaction has been studied using an Open Ended Shock Tube and droplets in the range [0.8-1.8] mm. Good agreements have been observed with Pilch and Erdmann theory. Mass median diameter of the fragments has thus been evaluated. Results show an increase of the total exchange surface during the fragmentation process from 81 to 108. Therefore, mass evaporation rate is expected to rise. If extended to the whole liquid jet, the total vapor phase fraction might reach important level that may require extra consequences analysis. More work has to be done on liquids involved in chemical or petrochemical processes. Moreover, fragmented droplet diameter will be evaluated using PDA techniques in future work.

Acknowledgments

This research was supported by the French Alternative Energies and Atomic Energy Commission (CEA, Commissariat à l'énergie atomique et aux énergies alternatives).

Reference

Dunbar, I.H., Hiorns, D.N., Mather, D.J., Tickle, G.A., 1984. Atomisation and dispersion of toxic liquids resulting from accidental pressurised releases, in: Hazards XII, European Advances in Process Safety. pp. 143–153.

Guella, S., Alexandrova, S., Saboni, A., 2008. Evaporation d'une gouttelette en chute libre dans l'air. Int. J. Therm. Sci. 47, 886–898. doi:10.1016/j.ijthermalsci.2007.07.020

Guildenbecher, D.R., López-Rivera, C., Sojka, P.E., 2009. Secondary atomization. Exp. Fluids 46, 371–402. doi:10.1007/s00348-008-0593-2

Hargather, M.J., Settles, G.S., 2009. Retroreflective shadowgraph technique for large-scale flow visualization. Appl. Opt. 48, 4449. doi:10.1364/AO.48.004449

Heymes, F., Aprin, L., Slangen, P., Lapébie, E., Osmont, A., Dusserre, G., 2014. On the Effects of a Triple Aggression (Fragment, Blast, Fireball) on an LPG Storage. Chem. Eng. Trans. 36, 355–360. doi:10.3303/CET1436060

Hsiang, L.-P., Faeth, G.M., 1995. Drop deformation and breakup due to the shockwave and steady disturbances. Int. J. Multiph. Flow 21, 545–560.

Joseph, D.D., Belanger, J., Beavers, G.S., 1999. Breakup of a liquid drop suddenly exposed to a high-speed airstream. Int. J. Multiph. Flow 25, 1263–1303. doi:10.1016/S0301-9322(99)00043-9

Lecysyn, N., Dandrieux, A., Heymes, F., Aprin, L., Slangen, P., Munier, L., Le Gallic, C., Dusserre, G., 2009. Ballistic impact on an industrial tank: study and modeling of consequences. J. Hazard. Mater. 172, 587–94. doi:10.1016/j.jhazmat.2009.07.086

Lee, C.H., Reitz, R.D., 2000. An experimental study of the effect of gas density on the distortion and breakup mechanism of drops in high speed gas stream. Int. J. Multiph. Flow 26, 229–244.

Pilch, M., Erdman, C.A., 1987. Use of breakup time data and velocity history data to predict the maximum size of stable fragments for acceleration-induced breakup of a liquid drop. Int. J. Multiph. Flow 13, 741–757.

Salzano, E., Cozzani, V., Kolbe, M., 2012. The interaction of accidental explosions with industrial equipment containing hazardous substances. Chem. Eng. Trans. 26, 159–164. doi:10.3303/CET1226027

Settles, G.S., 2001. Schlieren and Shadowgraph Techniques, Springer Berlin. doi:10.1007/978-3-642-56640-0

Slangen, P., Aprin, L., Heymes, F., Munier, L., Lapébie, E., Dusserre, G., 2012. Overpressure wave interaction with droplets: time resolved measurements by laser shadowscopy, in: Speckle 2012: V International Conference on Speckle Metrology. pp. 1–6. doi:10.1117/12.978639

Slangen, P., Lauret, P., Aprin, L., Heymes, F., Lecysyn, N., 2015. Optical characterizations of falling droplets interacting with shockwave, in: 10th Pacific Symposium on Flow Visualization and Image Processing. pp. 1–12

Slangen, P., Lauret, P., Heymes, F., Aprin, L., Lecysyn, N., 2016. High speed imaging optical techniques for shockwave and droplets atomization analysis, Optical Engineering 55 (12), 1-18